

Article

Growth and Distribution of Coal-Measure Source Rocks in Mixed Platform: A Case Study of Carboniferous in Bamai Area, Southwest Tarim Basin, China

Siyu Su ^{1,2}, Yongqiang Zhao ³, Renhai Pu ^{1,2,*}, Shuo Chen ^{1,2}, Tianyu Ji ⁴  and Wei Yao ³¹ State Key Laboratory of Continental Dynamics, Northwest University, Xi'an 710069, China² Department of Geology, Northwest University, Xi'an 710069, China³ SINOPEC Key Laboratory of Petroleum Accumulation Mechanisms, Wuxi Research Institute of Petroleum Geology, Wuxi 214126, China⁴ Research Institute of Petroleum Exploration and Development, PetroChina, Beijing 100083, China

* Correspondence: purenhai@nwu.edu.cn

Abstract: Coal-measure source rocks are generally developed in marsh facies under a humid climate and are rarely reported in a carbonate platform or a mixed platform. Carboniferous seawater intruded from west to east in the Tarim Basin, and mixed platform deposits of interbedded mudstone and carbonate developed in the southwest of the basin. In recent years, with the deepening of the exploration, nearly 20 m coal seams and carbonaceous mudstone source rocks have been found in the Carboniferous lagoon's tidal-flat background. The hydrocarbon generation potential, development, and distribution of these coal-measure source rocks have become an important issue for oil and gas exploration. Coal seams and carbonaceous mudstones were found in the Carboniferous formation of wells BT5, BT10, and Lx2. The hydrocarbon prospect, development, and distribution characteristics of these coal formations have become an important research topic. The authors conducted organic geochemical tests and analyses of core and samples drill cuttings from multiple wells in the study area, combined with research focused on the identification and distribution of coal seams, dark mudstones, and depositional facies via logging cross plots of different lithology and 3D seismic inversion. The results show that coal-measure source rocks in the BT5 well are related to the set of delta-lagoon sedimentary systems widely developed in the Carboniferous Karashayi Formation. The maximum cumulative thickness of coal-measure source rocks is about 20 m, with total organic carbon (TOC) contents of 0.15–60%, kerogen types II₂–III, and vitrinite reflectance (Ro) values of 0.78–1.65%. The rocks have generally low maturity in the northwestern area and high maturity in the southeastern area, and the maturity changes as the burial depth changes. The effective hydrocarbon source rocks such as coal, carbonaceous mudstone, and dark mudstone all show acoustic time (AC) greater than 300 μs/m, and density (DEN) less than 2.3 g/cm³, but possess different gamma ray (GR) values. The GR value is less than 75 API for coal, between 75–100 API for carbonaceous mudstone, and greater than 100 API for dark mudstones. The distribution of source rocks can be identified in the area between the wells according to a 3D seismic inversion impedance (IMP) of less than 7333 m/s·g/cm³. The development and controlled factors of coal-measure source rocks of delta facies in the mixed platform have a significant role for oil and gas exploration of Upper Paleozoic in this area. The coal measure and sandstones of delta in the Carboniferous are expected to form self-generation and self-storage pools in this area.

Keywords: Tarim Basin; mixed platform; delta; coal-measure distribution; coal-measure logging response

1. Introduction

The Carboniferous system in the Tarim Basin is generally composed of mixed platform deposits consisting of multiple cycles of carbonate rocks and mudstones (Figure 1c).



Citation: Su, S.; Zhao, Y.; Pu, R.; Chen, S.; Ji, T.; Yao, W. Growth and Distribution of Coal-Measure Source Rocks in Mixed Platform: A Case Study of Carboniferous in Bamai Area, Southwest Tarim Basin, China. *Energies* **2022**, *15*, 5712. <https://doi.org/10.3390/en15155712>

Academic Editors: Gan Feng, Qingxiang Meng, Gan Li and Fei Wu

Received: 14 June 2022

Accepted: 3 August 2022

Published: 5 August 2022

Publisher's Note: MDPI stays neutral with regard to jurisdictional claims in published maps and institutional affiliations.



Copyright: © 2022 by the authors. Licensee MDPI, Basel, Switzerland. This article is an open access article distributed under the terms and conditions of the Creative Commons Attribution (CC BY) license (<https://creativecommons.org/licenses/by/4.0/>).

From bottom to top, the Carboniferous is composed of 10 stratigraphic members: the Glutenite, Lower Mudstone, Bioclastic Limestone, Middle Mudstone, Standard Limestone of Bachu Formation, Upper Mudstone, Sand–Mudstone, Limestone-Bearing Member of the Karashayi Formation, and Limestone Member of the Xiaohaizi Formation [1,2]. Compared with the central and northern Tarim Basin, the terrigenous clastic proportion in the Carboniferous sediments in the southwest Tarim Basin (SWTB) decreases, and the carbonate content in the mudstone members increases. Furthermore, limestone rocks in the latter atypically contain partial dolomites and rare gypsum [3]. The proportion of carbonate rocks in the Karashayi Formation is a little higher, and coal seams are generally not developed [4,5]. However, multiple layers of coal seams and carbonaceous mudstones occurred in the Karashayi Formation in the BT5 well’s seismic survey, suggesting different sedimentary environments and hydrocarbon-generation potential from other areas of the basin. Therefore, it is meaningful to clarify the geochemical features, depositional environment, and distribution of the coal-source rocks.

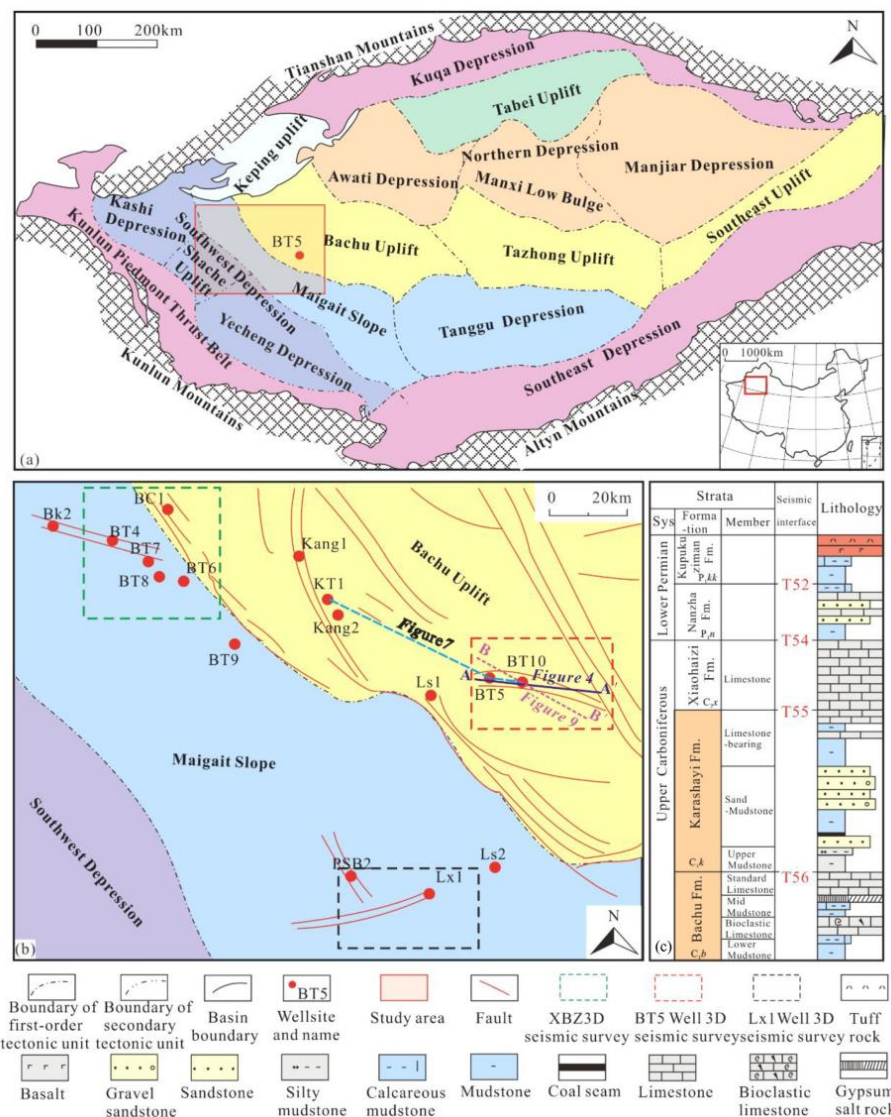


Figure 1. (a) The location map of the study area and the division of basin structural units in the Tarim Basin; (b) structural units map of the Bamai area, location map of 3D seismic survey, and (c) a comprehensive stratigraphic histogram from Carboniferous to Permian in the Bamai area; in (b), the green area is the XBZ 3D seismic survey, the red area is the Lx1 well 3D seismic survey, and the black area is the BT5 well 3D seismic survey. In (c), the orange area is the target formation.

The Cambrian–Lower Ordovician marine source rocks and the Carboniferous–Lower Permian marine–continental transitional source rocks are present in the Bachu Uplift and Maigaiti slope (abbreviated as the Bamai area) in the SWTB [6–9]. Previous studies have found that the Cambrian–Lower Ordovician source rocks are of high quality [10–13], while research on the Carboniferous source rocks in the Bamai area is relatively rare. Su et al. [14] and Huo et al. [15] conducted oil–source correlation by using carbon isotopes, biomarker compounds, and hydrocarbon components. They concluded that the Bashto light oil mainly formed in the Cambrian, and a small amount may have originated from Carboniferous carbonate and mudstone, as the maturity of the crude oil was obviously higher than that of the Carboniferous source rocks. Shen et al. [16] considered that the two types of source rocks, namely, Carboniferous mixed shelf mudstone and carbonate, contain type II organic matter and are in the overmature evolution stage. Du [17] considered that the Cretaceous oil and gas in well KD1 in the Kunlun Mountains originated from Carboniferous–Permian type II argillaceous mature source rocks in the eastern sag of the SWTB; the TOC contents are 0.04% and 4.19%, respectively, the maximum pyrolysis temperature (T_{max}) values are 400–595 °C, and the overall maturity and abundance of organic matter are high. Based on a large number of outcrops and borehole data, Chen et al. [18] mainly studied the lagoon facies argillaceous source rocks of the Karashayi Formation in the Macan 1 well. The source rocks of the Mazhatage structural belt centered on the Macan 1 well were considered to be approximately 60 m, with low to medium maturity and relatively limited distribution.

Based on outcrops and limited drilling data, predecessors mainly studied two types of hydrocarbon source rocks: Carboniferous carbonate rocks and mudstones. Coal-measure source rocks were not been involved, and, furthermore, less attention was paid to the middle and lower mudstones of the Bachu Formation. The methods of logging, seismic attribute [19,20], inversion [21,22], and geochemical analysis are, hereby, used to comprehensively analyze and evaluate the characteristics of hydrocarbon source rocks [23,24]. The well logging and seismic data are used to determine the depositional facies and distribution of hydrocarbon-source rocks [25,26]. This study focuses on the coal seams and carbonaceous mudstones found in the Carboniferous Karashayi Formation in well BT5. The geophysical methods of discriminating different coal-measure source rocks are explored by using well logging and 3D seismic data. At the same time, the seismic facies, depositional environment, and their control over the coals of Karashayi Formation have been analyzed, which provides geological evidences for finding oil and gas reservoirs related to coal-measure source rocks.

2. Geology of the Study Basin

The Tarim Basin is a composite petroliferous basin with an area of approximately 56×10^4 km² [27]. The study area is located in two structural units of the Bachu uplift and Maigaiti slope in the southwestern Tarim Basin, China, which is referred to as the Bamai area (Figure 1a). The Bamai area is bordered by the Keping uplift to the north; the northern depression and Tazhong uplift to the east; and the Kashi sag, Shache uplift, and Yecheng sag to the southwest [28–31]. The Carboniferous strata are one of the main subjects of oil and gas exploration in the Bamai area and contain the Bachu Formation, Karashayi Formation, and Xiaohaizi Formation from the bottom up. Under the action of dry and wet climate alternation and the rise and fall of relative sea level, a deep-water shelf, shallow-water shelf, lagoon bay, delta, and other sedimentary environments were mainly developed [32–37]. The main lithologies include limestone, dolomite, marlstone, mudstone, etc., and these lithologies are partially intercalated with gypsum dolomite and gypsum mudstone and locally embedded with coal seams, gypsum dolomite, and gypsum mudstone [38,39]. Years of exploration have shown that the Carboniferous rocks have the capability of hydrocarbon generation, storage and capping [40]. The coal-measure source rocks seen first in the delta environment are related to the Carboniferous mixed platform.

3. Data and Methods

The study area contains 15 exploration wells, 18 2D seismic lines, and 3 3D seismic surveys (Figure 1a), of which the 3D seismic surveys are XBZ 3D seismic surveys (approximately 600 km²), Lx1 well 3D seismic survey (approximately 350 km²), and BT5 well 3D seismic survey (approximately 400 km²). The main frequency of the 3D seismic data is approximately 35 Hz, the sampling rate 2 ms, trace interval 25m, the sampling length 0–6000 ms, and the datum elevation 1000 m. All the seismic data were processed as poststack volumes processed through high resolution, high signal-to-noise ratio, and high relative-amplitude preservation. There are 9 wells in the 3D seismic surveys, most wells drilled through the bottom of Upper Paleozoic, with total depth over 4000 m, a few wells have core data of Carboniferous, and each well contains comprehensive logging curves, including gamma ray (GR), resistivity (RD), acoustic time (AC), neutron (CN), density (DEN), etc., with sample rate 0.125 m. Upper Paleozoic revealed by drilling in the area includes Permian Kupukuzman Formation (P₁kk), Nanzha Formation (P₁n), Xiaohaizi Formation (C₂x), Carboniferous Karashayi Formation (C₁k), and Bachu Formation (C₁b), with bottom seismic reflection interfaces that are T52, T54, T56, and T57, respectively (Figure 1c).

Except for the coring of coal measure in the Karashayi Formation of well BT5, most of the samples of Carboniferous source rocks are drilling cuttings. The coring section of the Karashayi Formation in well BT5 is 2077.5–2084 m, and the lithology from top to bottom is gray black carbonaceous mudstone and dark gray mudstone containing light gray silty strip, with local plant fragments (Figure 2). Coal samples come from drilling cuttings, which are dark black, small, granular, glassy, and stained, and their final affirmatory lithology is determined by subsequent geochemical tests for organic matter.

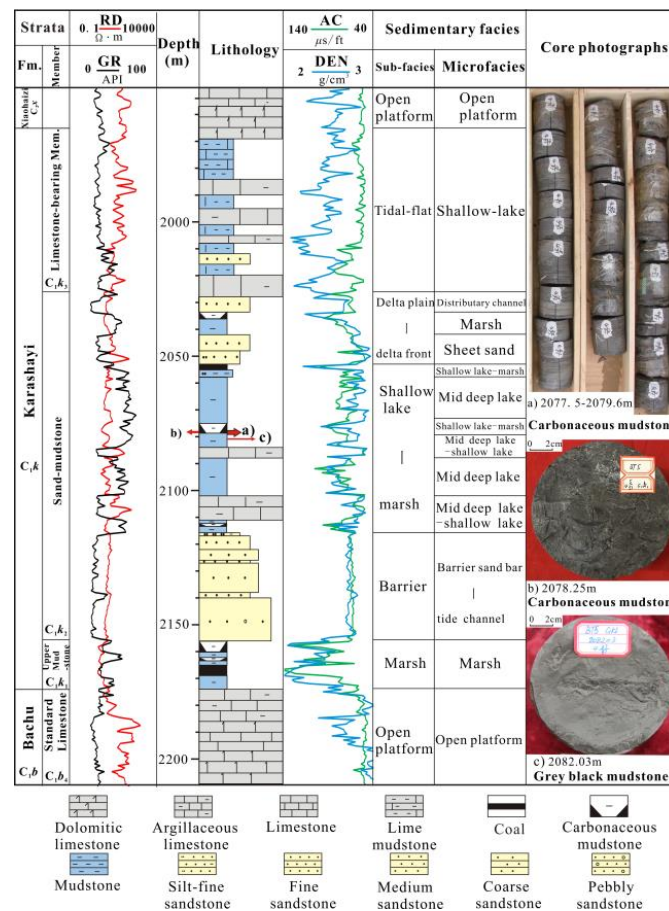


Figure 2. A comprehensive stratigraphic profile of the Carboniferous Karashayi Formation of well BT5.

Based on the core, logging, and cutting data of BT5 and BT10 wells in the work area, cross plots of AC-GR and DEN-RD to differentiate lithologies are established. The threshold values for quantitative identification of coal seams, carbonaceous mudstone, shale, sandstone, and carbonate rocks are determined. Then, synthetic seismograms of two wells, BT5 and BT10, are made, well seismic calibration is completed, and log-constrained poststack wave impedance inversion is carried out in the 3D seismic survey of BT5. In the invertomer, the content and thickness percentages of the related lithologies of the Karashayi Formation are extracted, according to the wave impedance of the coal seam, carbonaceous mudstone, and sandstone.

In addition, 30 samples of Carboniferous cores and drilling cuttings are collected from Sinopec; in particular, these samples include coal, carbonaceous mudstone, and dark mudstone from wells BT5, BT10, and BT7. After sample separation and selection of different lithologies, 12 samples of drill cuttings and 2 core samples from the Carboniferous Karashayi and Bachu Formations are obtained. The organic matter extraction and pyrolysis experiments of all 14 samples are carried out in the State Key Laboratory of Continental Dynamics of Northwestern University, and the organic carbon content, type, and maturity of each sample are determined (Table 1).

Table 1. TOC, Ro, and organic carbon type of hydrocarbon source rock samples from the Carboniferous Karashayi Formation and Bachu Formation.

Number	Well	Stratum	Sample Type	Depth (m)	Lithology	T _{max} (°C)	TOC (%)	Ro	Organic Carbon Type
1	BT5	C ₁ k ₂	Core	1918.1	Carbonaceous mudstone	437	14.2	1.65	III
2	BT5	C ₁ k ₂	Core	1917.6	Mudstone	434	0.15	0.90	III
3	KT1	C ₁ k ₂	Cuttings	1620	Carbonaceous mudstone	431	14.4	0.78	II ₂
4	BT5	C ₁ k ₂	Cuttings	2040	Carbonaceous mudstone	424	10.6	0.78	II ₂ -III
5	BT10	C ₁ b ₁	Cuttings	2660	Mudstone	436	0.01	0.80	III
6	BT7	C ₁ k ₂	Cuttings	4520	Mudstone	431	0.01	0.97	III
7	BT7	C ₁ k ₂	Cuttings	4540	Mudstone	428	0.86	1.33	III
8	BT9	C ₁ k ₂	Cuttings	4740	Mudstone	437	1.15	1.13	III
9	BT5	C ₁ k ₁	Cuttings	2020	Mudstone	428	2.36	0.87	III
10	BT5	C ₁ k ₂	Cuttings	2095	Mudstone	432	0.94	0.80	III
11	BT5	C ₁ b ₃	Cuttings	2400	Mudstone	429	0.15	/	III
12	BT5	C ₁ k ₂	Cuttings	2055	Coal	425	58.1	1.29	II ₁ -II ₂
13	BT5	C ₁ k ₂	Cuttings	2060	Carbonaceous mudstone	424	18.5	0.81	II ₂
14	KT1	C ₁ k ₂	Cuttings	1605	Coal	432	63.2	0.93	III

By plotting the Ro value and well depth of source rock samples measured in different wells, the trend of source rock maturity with target layer depth in the study area is obtained. The trend is then extrapolated to the structural map of the bottom of the Karashayi Formation to estimate the maturity of the source rocks of the said formation in the Bamai area.

4. Results

4.1. Logging Identification of Carboniferous Source Rocks

Logging curves calibrated by the core (Figure 2) and AC-GR cross plot (Figure 3) indicate that coal and dark mudstone have logging responses of low DEN, high AC, and low RD values [41], and their AC values are all more than $300 \mu\text{s}/\text{m}$, the DEN value is generally less than $2.2 \text{ g}/\text{cm}^3$, and the RD value is less than $50 \Omega\cdot\text{m}$; they are easy to be identified in logging curves because of their high-amplitude spikes. Coal, carbonaceous mudstone, and dark shale can be distinguished by GR values. The GR values are <75 API for coal seam, between 75 and 100 API for carbonaceous mudstone, and >100 API for dark mudstone. According to the above logging identification method, two coal seam layers are present in the BT5 well, with a cumulative thickness of approximately 6 m; five layers of carbonaceous mudstone are present with a cumulative thickness of approximately 10 m; and nine layers of dark mudstone are present with a total thickness of approximately 66 m, of which coal seams and carbonaceous mudstone account for 24.2%. The sandstone shows a box-shaped GR logging curves [42], with $\text{AC} < 240 \mu\text{s}/\text{m}$ and $\text{GR} < 60$ API, and $\text{RD} < 100 \Omega\cdot\text{m}$, which is much less than the RD values of carbonate rocks (Figure 3).

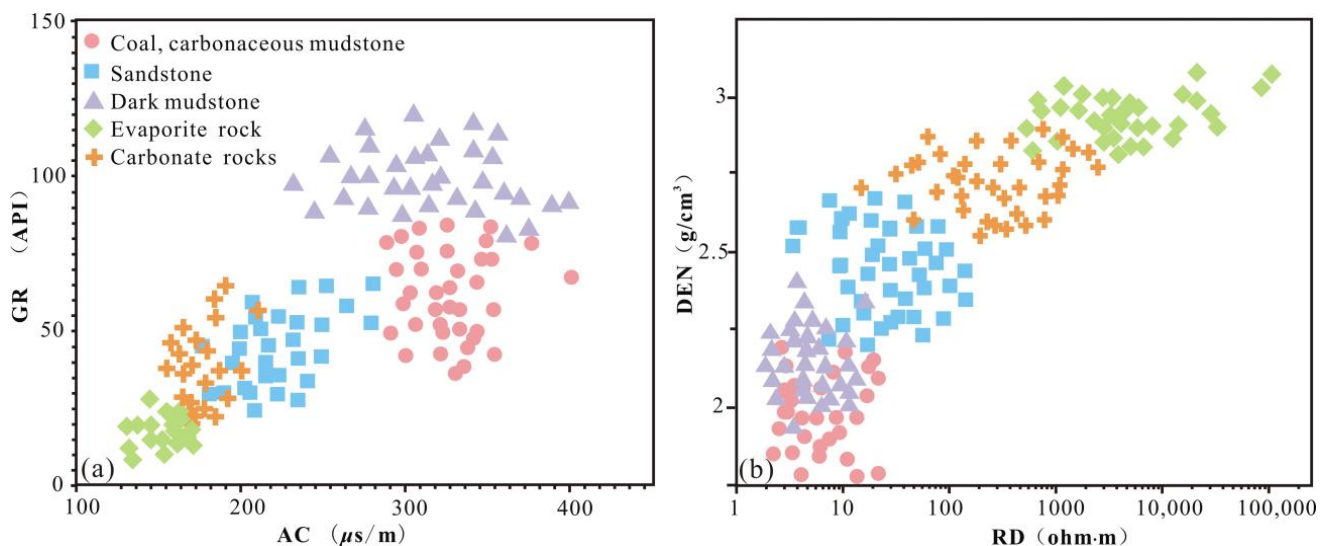


Figure 3. Log cross plots of different lithologies of the Karashayi Formation in the Bamai area. (a) AC-GR cross plot. (b) DEN-RD cross plot.

4.2. 3D Seismic Identification and Distribution of Coal-Measure Source Rocks in the Karashayi Formation

In order to identify coal-measure source rocks with 3D seismic data, we have performed log constrained 3D seismic impedance inversion. Figure 4 is the BT5–BT10 well-linked inversion acoustic section. There is a bright yellow banded layer between seismic interfaces from T52 to T54 that corresponds to a large set of low-speed mudstone and tuff widely distributed in the lower Permian. The seismic interface from T55 to T56 corresponding to the Carboniferous Karashayi Formation, with an AC value of $200\text{--}350 \mu\text{s}/\text{m}$, about 10–40 ms thick, in which the part of $\text{AC} > 300 \mu\text{s}/\text{m}$ should belong to coal-measure source rocks, and they gradually thicken to the southeast lower part of the depression.

According to the logging and seismic-identification threshold values of coal seam and carbonaceous mudstone of the Karashayi Formation in the study area (the $\text{AC} > 300 \mu\text{s}/\text{m}$, $\text{DEN} < 2.2 \text{ g}/\text{cm}^3$, and $\text{Imp} < 7333 \text{ m}/\text{s}\cdot\text{g}/\text{cm}^3$), the percentage content of wave impedance less than $7333 \text{ m}/\text{s}\cdot\text{g}/\text{cm}^3$ in the Karashayi Formation can be extracted from the 3D seismic-wave impedance inversion volume as the percentage map of coal-measure source rocks (Figure 5). The map indicates that the coal and carbonaceous mudstone are thickening to the southeast.

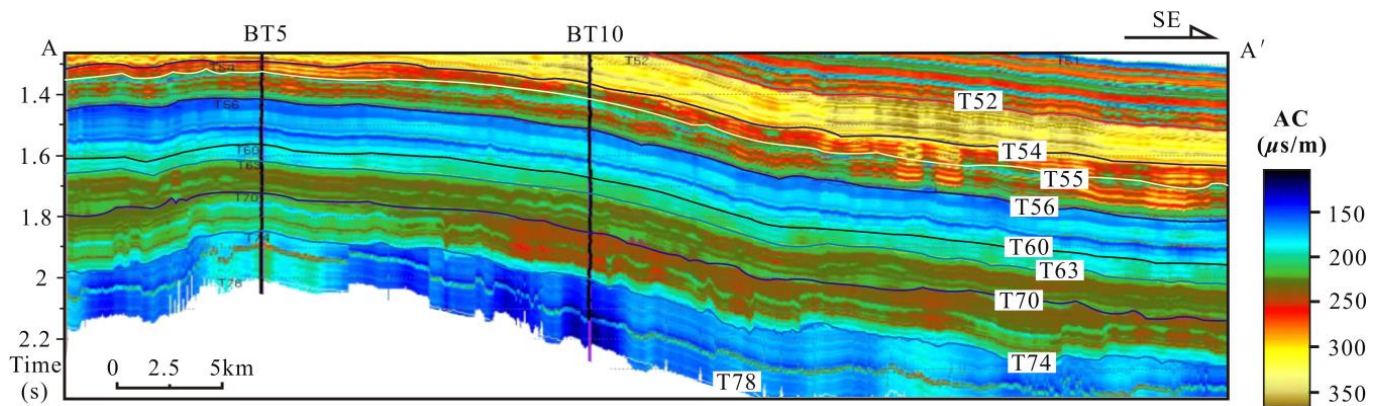


Figure 4. BT5–BT10 well-linked 3D seismic inversion acoustic profile. See Figure 1b for section position.

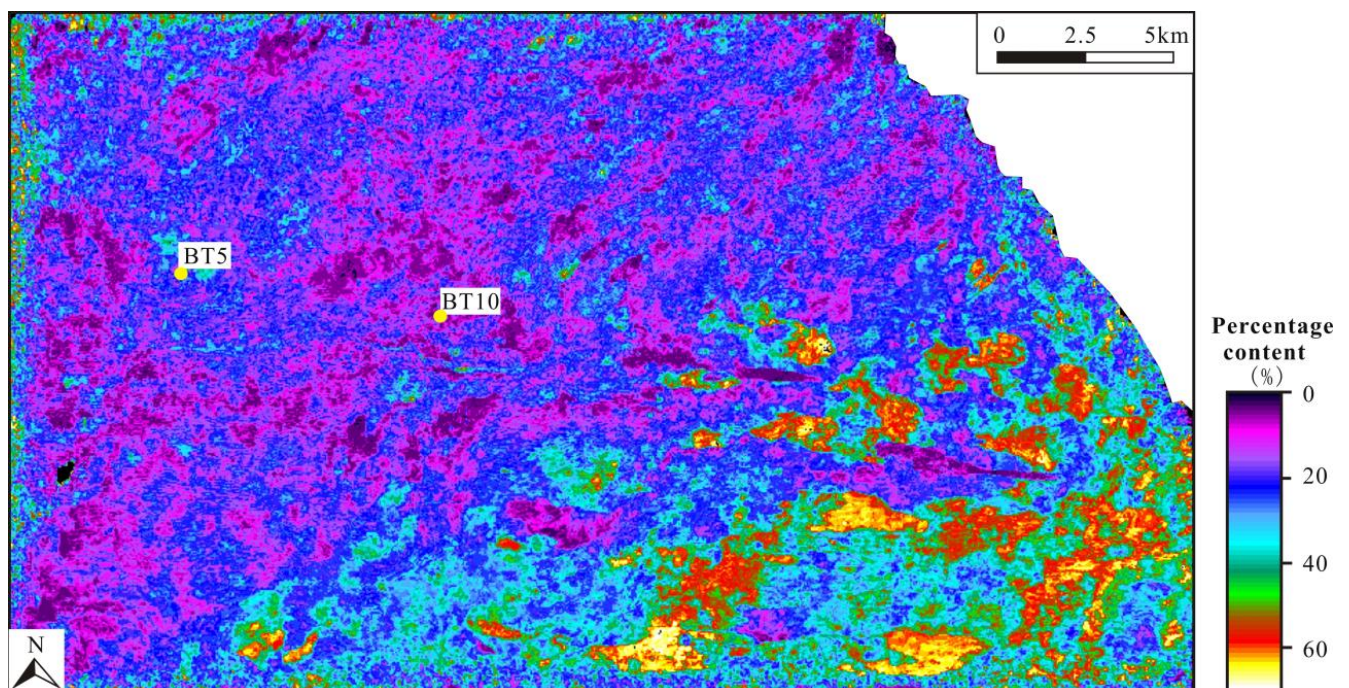


Figure 5. Percentage contents of coal and carbonaceous mudstone in the Karashayi Formation in the BT5 well 3D seismic survey.

Using the SUM module of landmark, the cumulative thickness of source rocks in the Karashayi Formation of the 13 drilling well points is counted, and, under the constraint of the percentage of coal seams, the carbonaceous mudstone and dark mudstone are obtained through 3D seismic inversion, so the contour map of the thicknesses of coal seams and carbonaceous mudstones in the study area is drawn (Figure 6). The map shows that the thicknesses of the coal-measure source rock of the Karashayi Formation in the study area are about 0–20 m and thicken from northwest to southeast. The area of thick coal-measure source rocks is about 40 km².

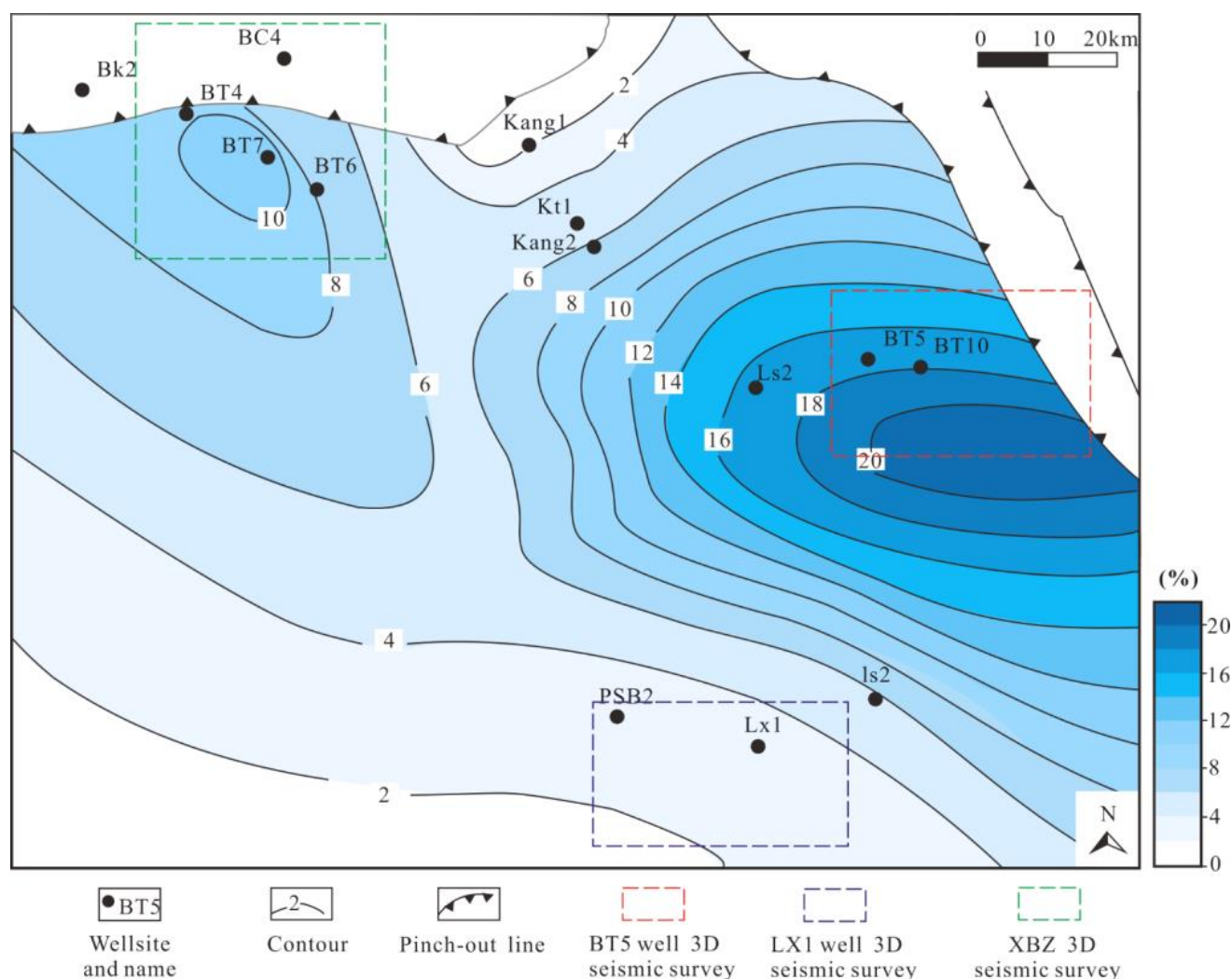


Figure 6. Isopach map of the cumulative thickness of the Carboniferous Karashayi Formation coal and carbonaceous mudstone in the Bamai area.

4.3. Geochemical Characteristics of Source Rocks

The test results of samples from wells BT5, BT10, KT1, BT7, and BT9 show that the TOC contents of the Karashayi Formation coal range from 58.1% to 63.2%, with an average of 60.65%, and the Ro values range from 0.93% to 1.29%, with an average of 1.11%. The TOC contents of carbonaceous mudstone range from 10.6% to 18.5%, with an average of 14.43%, and the Ro values range from 0.78% to 1.65%, with an average of 1.00%. The TOC contents of dark mudstone range from 0.01% to 2.36%, with an average of 0.91%, and the Ro values range from 0.80% to 1.33%, with an average of 1.00%. According to the calculation results of the hydrogen index–Tmax diagram [43], the organic carbon types of most coal seams and carbonaceous mudstones are of type III, and some carbonaceous mudstones are of types II₂–III (Table 1).

Based on the test results of the Carboniferous Karashayi Formation coal and dark mudstone, the TOC content is between 0.17% and 63.2%, the types of organic carbon are II₂–III, and the Ro values are 0.78–1.65% for coal and dark mudstone of the Carboniferous Karashayi Formation. The Tmax values range from 424 °C to 437 °C, with an average of 430 °C, indicating oil generation of immature to low maturity, which are slightly lower than the maturity indicated by the Ro values.

The preliminary sample separation and selection revealed that most of the samples collected from the Middle and Lower Mudstone Members of the Carboniferous Bachu Formation do not meet the requirements of pure dark mudstone, are not distinguishable from

dry drilling mud, or are oxidized brown. Only two samples from the Middle and Lower Mudstone Members meets the test conditions (see Yellow Sampling Points in Figure 7). Test shows that the TOC contents of the dark shale in the Middle and Lower Mudstone Members of the Carboniferous Bachu Formation are low, ranging from 0.01–0.15%, with an average of 0.08%, which does not meet the conditions for hydrocarbon generation (Table 1).

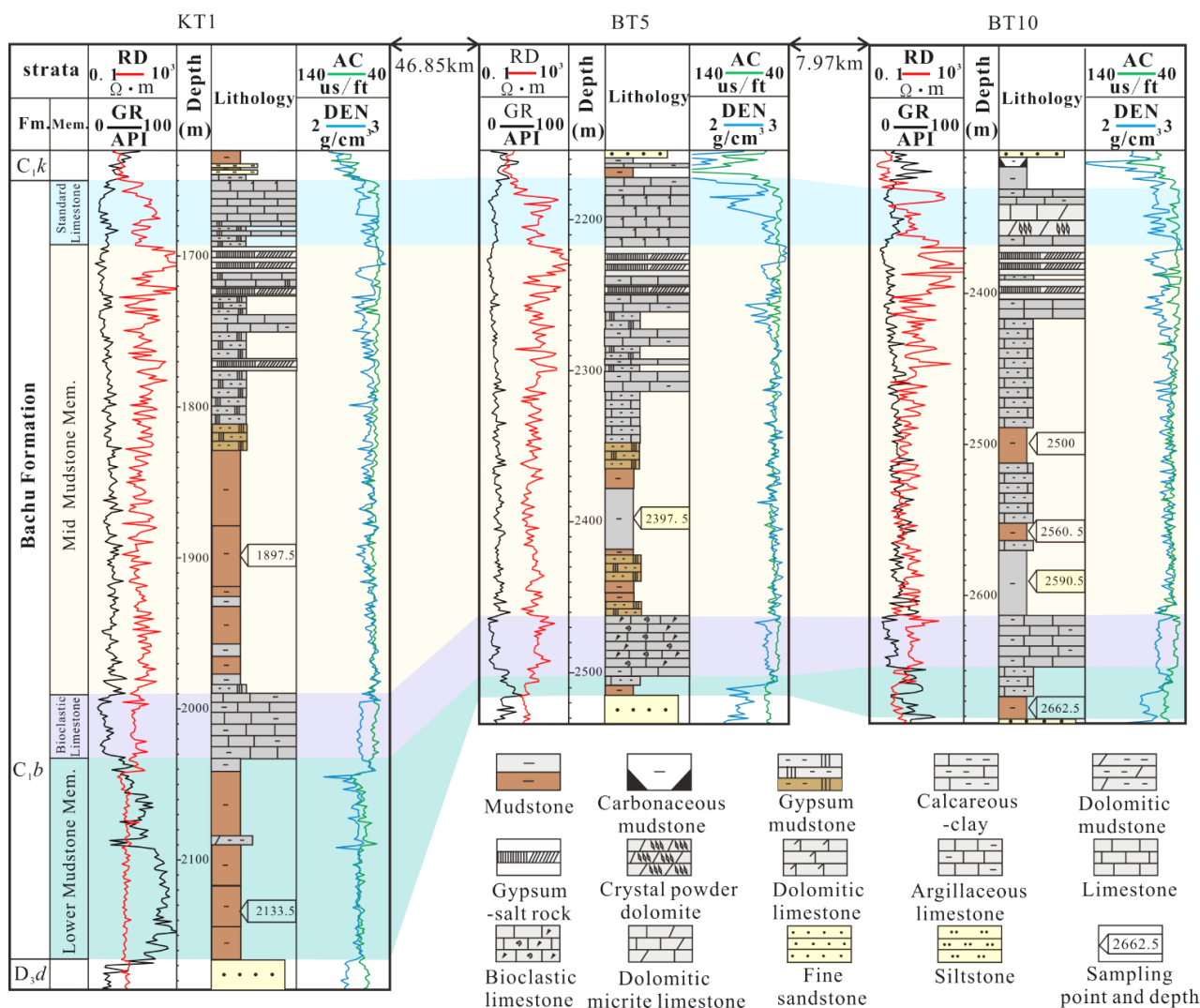


Figure 7. Profile of wells KT1, BT5, and BT10 of the Bachu Formation. See Figure 1b for the lateral positions. In the legend, the different colors filled by mudstone and gypsum mudstone reflect different sedimentary backgrounds, in which brown represents the oxidation environment and gray represents the reduction environment.

In Table 1, the linear relationship of $Ro = 0.0001H + 0.622$ between the Ro and sample depth (H) is obtained by linear fitting. The depth map of the bottom boundary of the Karashayi Formation in the Bamai area can be made through the two-way time map of the seismic interface T56 and the time–depth conversion of the Karashayi Formation. By using the linear relationship of Ro – H , the depth map of the top surface of the Karashayi Formation can be transformed into a contour map showing vitrinite reflectance (Figure 8). The map shows that the Ro value of the source rock of the Karashayi Formation in the Bamai area is between 0.7% and 1.3%, which has a tendency to increase toward the southwest.

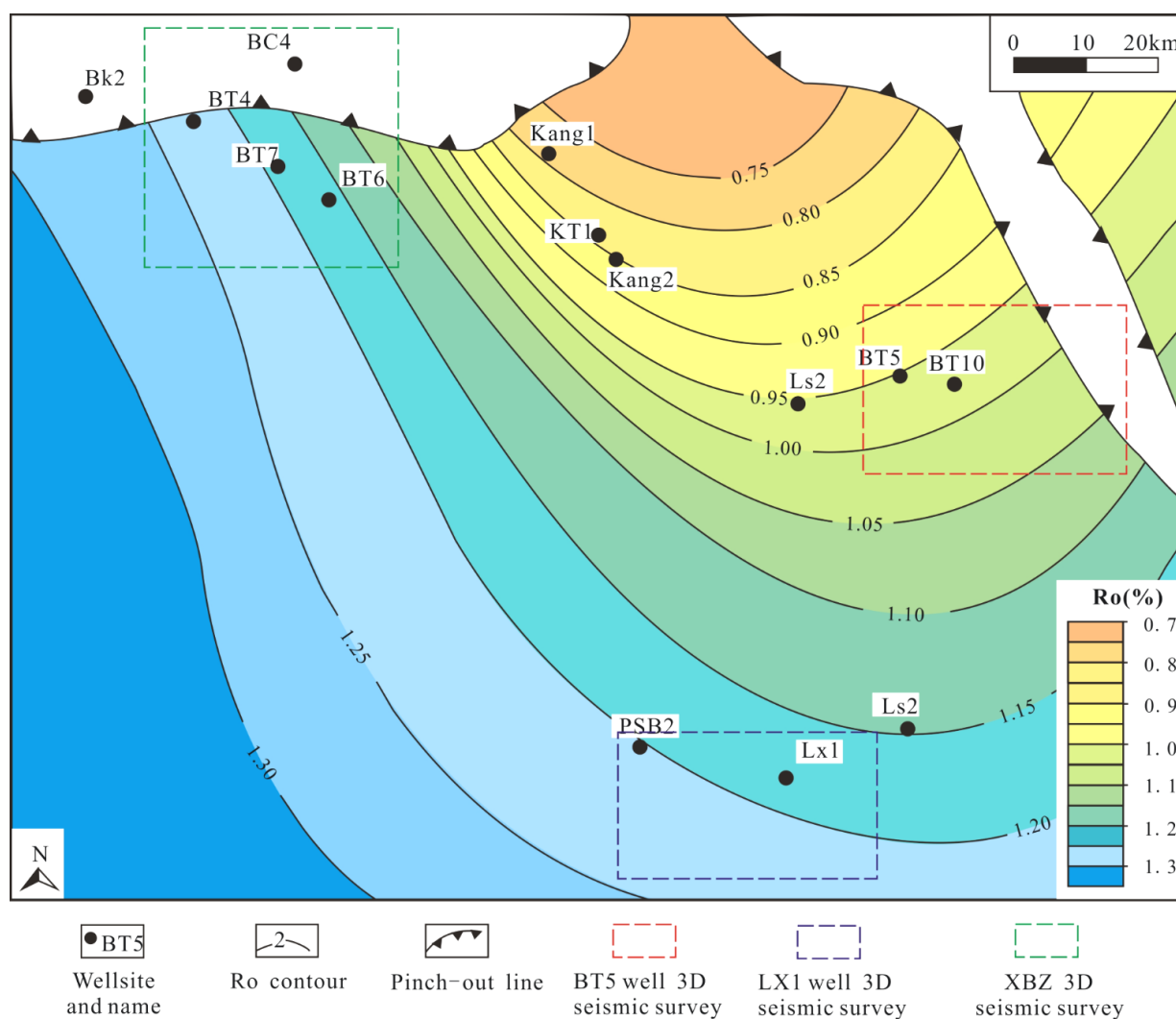


Figure 8. Vitrinite reflectance Ro contour map of the bottom Carboniferous Karashayi Formation in the Bamai area.

4.4. Deltaic Control on Coal-Measure Source Rocks

A set of imbricated progradational reflection can be identified in the Carboniferous Karashayi Formation of the BT5 3D seismic survey, which advances from northwest to southeast. The set is prograded by the phase axes of five progradational wave peaks with medium and strong amplitudes, representing the five stages of progradational sedimentary bodies (Figure 9). The progradational reflections can exist in a variety of sedimentary environments [44]. The seismic reflections of the five-stage progradation are traced, interpreted, and closed in detail in the BT5 well 3D seismic survey, and the plane distribution of the five stage progradation is obtained (Figure 10). BT5 and BT10 are located on the first and the second progradational leaves, respectively, and they correspond to the delta-front facies, with the upward coarsening of the Karashayi Formation (Figure 2). Based on the regional drilling data and previous studies [45], this delta system was developed in the lagoon sedimentary background and surrounded by a tidal flat and barrier system.

Sandstone content has a relatively sensitive response to sedimentary microfacies, and is an important means to study depositional facies and sand-body distribution rules [23,24]. Different sandstone content can reflect different sedimentary environments. Based on the data of 13 wells situated in the Bamai area, the percentage content of sandstone in the Karashayi Formation was estimated, and its depositional facies map was made accordingly (Figure 11). Due to the limited number of wells in the study area, the sandstone content is linearly extrapolated in the non-drilled area (such as the southwest area), so the depo-

sitional facies are not described in detail, but the genesis, distribution, and identification of coal-measure source rocks are focused in the general context of clarifying that the depositional facies is a mixed platform-lagoon tidal-flat environment. The study area is a lagoonal sedimentary setting overall, in which three delta front lobes from the northwest are developed, and the percentage of sandstone in the delta is high, ranging from 25% to 45%. The depositional facies in the western part of the study area are transitional to the mixed platform and the tidal-flat subfacies.

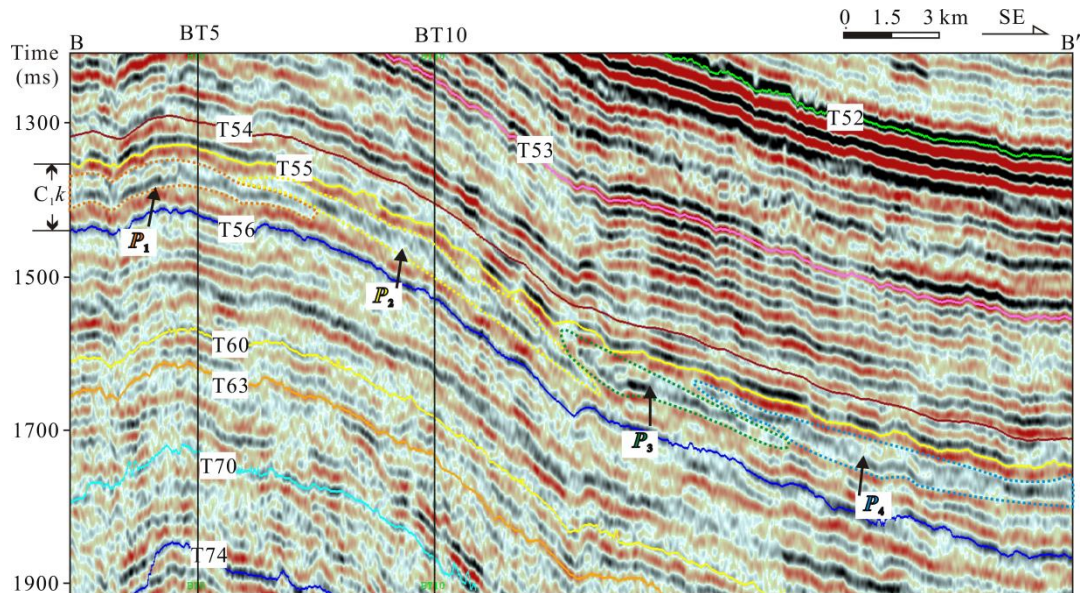


Figure 9. Seismic section across wells BT5 and BT10 in SE direction of the delta progradational reflection of the Karashayi Formation. See Figure 1b for section position, P_1 means progradation I, P_2 means progradation II, P_3 means progradation III, and P_4 means progradation IV. Karashayi Formation is located between T55–T56 seismic reflection boundaries. See Figure 1b for the location.

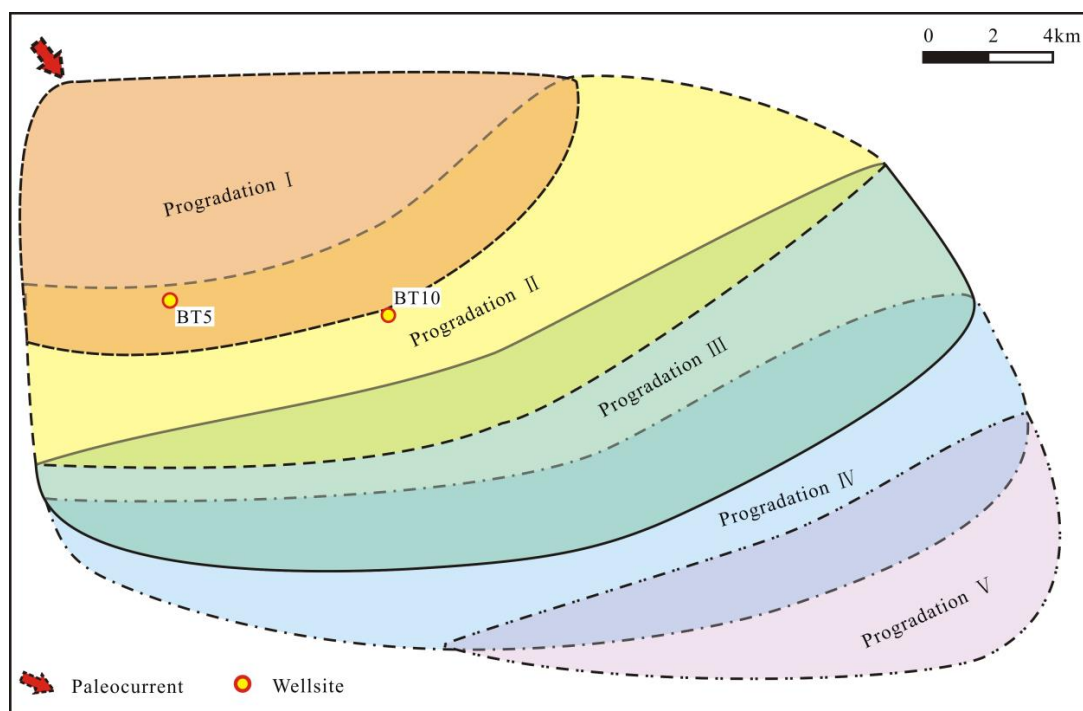


Figure 10. Superposition map five-stage progradational reflections in five different semitransparent colors.

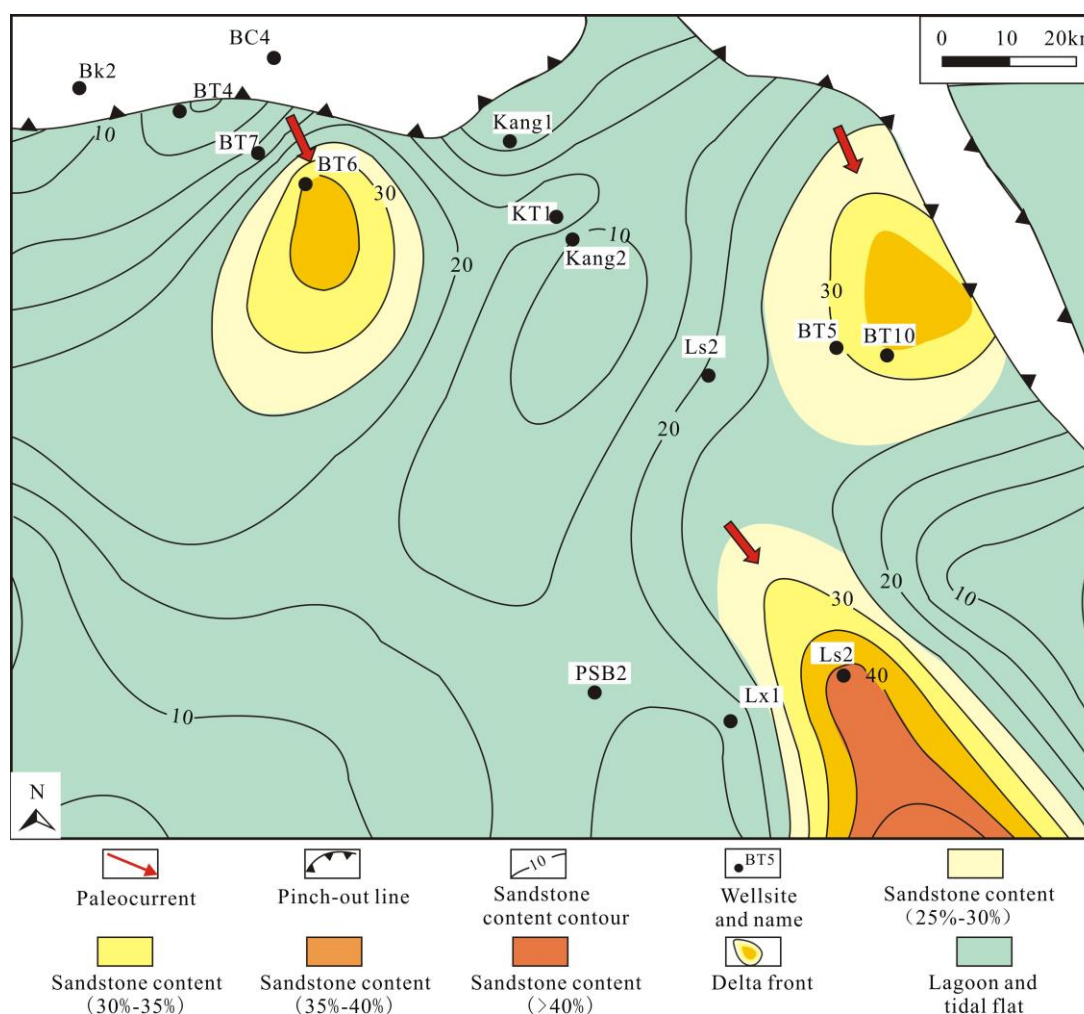


Figure 11. Depositional facies map of the Carboniferous Karashayi Formation in the Bamai area.

5. Discussion

5.1. Relationship between the Coal-Measure Source Rocks and Deltas in the Background of Mixed Platform

A comparison of Figures 7 and 11 shows that the thicker area of the coal-measure source rocks in the Bamai area is basically consistent with the distribution area of the delta front; this result indicates that in the lagoonal sedimentary background of the Karashayi Formation as a whole in the southwestern Tarim Basin area, there was an inflow of a freshwater river from the northwest in the BT5 well 3D seismic survey, and different progradational deltas were accumulated gradually from northwest to southeast. This process formed not only sandstone deposits, such as an estuary bar and distributary channels in the delta front, but also a certain thickness of swamp coal and carbonaceous mudstone on the delta plain. Since the organic matter contents of coal and carbonaceous mudstones are much higher than those of lagoon facies' dark mudstones, the coal-measure source rocks in the delta sedimentary area should have better hydrocarbon-generation potential than other surrounding areas.

Coal seams are commonly found in clastic strata and deposited in swampy environments in humid climates [46]. The Carboniferous in the Tarim Basin contains interbedded arid and semi-arid carbonate rocks and mudstones, with local gypsum salts, and no coal developed in other parts of the basin or the surrounding outcrops. Therefore, the Karashayi Formation coal seams in the BT5 well 3D seismic area are a special case, and their formation and distribution should be related to the freshwater delta that occurred locally in the mixed platform. Carbonate rocks are deposited in clear, warm, and full sunlight in a shallow

water environment, while mudstone and gypsum mudstone are deposited in hot and turbid shallow water or a tidal-flat environment [47]. The local existence of a delta makes the water bodies less saline, becoming turbid, which weakens the sedimentation of the carbonate rock and evaporated salt rock and increases the proportion of local sand–mud sediment in the background of the mixed platform. In addition, the fresh water body of the delta plain is beneficial to the growth of vegetation to form coal measures. The upward coarsening cycles of Carboniferous Karashayi Formation in the BT5 well and the typical imbricate progradational reflections in the 3D seismic survey verify the existence of deltas. The low seismic-inversion impedance shows that coal seams are also thickened in the delta sedimentary area, further suggesting the close relationship between the origin and distribution of coal measures and the delta in this area.

5.2. Potential of the Coal-Measure Source Rocks in Bamai Area

Many years of exploration practice and previous studies have shown that the Cambrian–Lower Ordovician source rocks provide oil and gas for the Ordovician gas fields such as Yubei, Hetian River, Niaoshan, BT5 well, etc., in the SWTB [32]. The Carboniferous source rocks in the Bamai area have a certain role in hydrocarbon generation and may be used as the minor source rocks of the Bashito and Yasundi oil and gas reservoirs. Two types of hydrocarbon source rocks were considered to exist in the Carboniferous: shallow-sea mixed continental-shelf mudstone and carbonate rock with low maturity, which only reached the maturity stage near well Kedong 1 in Kunlun Mountains, while coal-measure source rocks were never found before [17]. Our study reveals that there is a set of good source rocks in the Bamai area, with the maturity increasing with burial depth, and the content of the organic carbon is much higher than that of the dark mudstone in the same stratum. Coal measures are of better hydrocarbon generation potential and, hopefully, are one of the main source rocks in this area like Cambrian shale.

5.3. Excellent Conditions for Self-Generation and Self-Storage Composite Reservoirs in Carboniferous

In the Bamai area, the oil and gas pools related to the Cambrian–Ordovician source rocks are distributed along the faults, which is a necessary passage for oil and gas migration vertically upward [12]. However, in the areas where Carboniferous high-quality coal-measure source rocks exist, reservoirs could be formed without fault passages. The high-quality coal source rocks of Carboniferous Karashayi Formation in Bamai area have a substantial thickness and wider distribution. They are vertically superposed and transversely contiguous to delta-front sandstones. The deltaic sand body is pinched out toward the upper northwest, satisfying the conditions to form stratigraphic traps. The oil and gas generated by coal-measure source rocks and delta sandstones constitute a beneficial source-reservoir-cap matching, trap, and migration condition. Therefore, the “self-generating, self-accumulating” reservoirs of the Karashayi Formation are expected to be an important exploration target in this area.

6. Conclusions

1. A set of coal and carbonaceous mudstone source rocks are revealed in the Karashayi Formation in the SWTB, China, with an average TOC content of 60.6% and 14.4%, respectively, for coal and carbonaceous mudstone, with types II₂–III kerogen, and Ro values of 0.78–1.65%.
2. The coal seam and carbonaceous mudstone of the Karashayi Formation are characterized by low DEN (<2.2 g/cm³), high AC (>300 μs/m), and low wave impedances (<7333 m/s·g/cm³). They can be roughly distinguished according to the natural gamma logging values less and greater than 75 API, respectively. The thicknesses of a single-layer coal seam drilled by wells are generally 1–4 m, the cumulative thickness is approximately 20 m plus carbonaceous mudstones, and the area of thick coal-measure source rocks is about 40 km².

3. The Karashayi Formation in the Bamai area is mainly a delta-lagoon deposit in a mixed-platform background. Coal and carbonaceous mudstone are mainly distributed along the delta system and thin toward the tidal-flat area in the west. The hydrocarbon potential of the coal-measure source rocks in the delta of the Karashayi Formation near well BT5 should be better than that in the adjacent area overall.
4. The Lower Mudstone Member and the Middle Mudstone Member of the Bachu Formation contain interbedded gray and variegated mudstones. The TOC contents of dark mudstones with single-layer thicknesses of more than 5 m are generally less than 0.3%, and the mudstones do not have the conditions for hydrocarbon generation.

Author Contributions: Writing—original draft, S.S., Y.Z., R.P., S.C., T.J. and W.Y. Conceptualization, R.P. and S.S.; methodology, S.S.; software, S.C.; validation, Y.Z., R.P. and S.S.; formal analysis, R.P.; investigation, S.C.; resources, Y.Z.; data curation, S.S.; writing—original draft preparation, S.S.; writing—review and editing, R.P.; visualization, S.S.; supervision, W.Y.; project administration, R.P.; funding acquisition, T.J. All authors have read and agreed to the published version of the manuscript.

Funding: This research was funded by “Reservoir forming conditions and zonal evaluation of Paleozoic Clastic Rocks in Tarim” grant number [No. p21049-2].

Acknowledgments: The authors thank the Sinopec Northwest Oilfield Branch for providing relevant 3D seismic and well data.

Conflicts of Interest: The authors declare no conflict of interest.

References

1. Ren, Q.Q.; Feng, J.W.; Johnston, S.; Zhao, L.B. The influence of argillaceous content in carbonate rocks on the 3D modeling and characterization of tectonic fracture parameters—example from the carboniferous and ordovician formations in the hetianhe gas field, Tarim Basin, NW China. *J. Pet. Sci. Eng.* **2021**, *203*, 108668. [[CrossRef](#)]
2. Fu, M.Y.; Song, R.C.; Gluyas, J.; Zhang, S.N.; Huang, Q. Diagenesis and reservoir quality of carbonates rocks and mixed siliciclastic as response of the Late Carboniferous glacio-eustatic fluctuation: A case study of Xiaohaizi Formation in western Tarim Basin. *J. Pet. Sci. Eng.* **2019**, *177*, 1024–1041. [[CrossRef](#)]
3. Zhu, G.Y.; Zhang, S.C.; Su, J.; Meng, S.C.; Yang, H.J.; Hu, J.F.; Zhu, Y.F. Secondary accumulation of hydrocarbons in Carboniferous reservoirs in the northern Tarim Basin, China. *J. Pet. Sci. Eng.* **2013**, *102*, 10–26. [[CrossRef](#)]
4. Geng, F.; Wang, H.X.; Hao, J.L.; Gao, P.B. Internal Structure Characteristics and Formation Mechanism of Reverse Fault in the Carbonate Rock, A Case Study of Outcrops in Xike'er Area, Tarim Basin, Northwest China. *Front. Earth Sci.* **2021**, *9*, 1166. [[CrossRef](#)]
5. Wu, X.Q.; Tao, X.W.; Hu, G.Y. Geochemical characteristics and source of natural gases from Southwest Depression of the Tarim Basin, NW China. *Org. Geochem.* **2014**, *74*, 106–115. [[CrossRef](#)]
6. Bian, L.H.; Liu, X.F.; Wu, N.; Wang, J.; Liang, Y.L.; Ni, X.E. Identification of High-Quality Transverse Transport Layer Based on Adobe Photoshop Quantification (PSQ) of Reservoir Bitumen: A Case Study of the Lower Cambrian in Bachu-Keping Area, Tarim Basin, China. *Energies* **2022**, *15*, 2991. [[CrossRef](#)]
7. Pang, X.Q.; Chen, J.Q.; Li, S.M.; Chen, J.F. Evaluation method and application of the relative contribution of marine hydrocarbon source rocks in the Tarim basin: A case study from the Tazhong area. *Mar. Petro. Geol.* **2016**, *77*, 1–18. [[CrossRef](#)]
8. Song, Z.H.; Tang, L.J.; Liu, C. Variations of thick-skinned deformation along tumuxiuke thrust in Bachu uplift of Tarim Basin, northwestern China. *J. Struct. Geol.* **2021**, *144*, 104277. [[CrossRef](#)]
9. Cui, H.F.; Tian, L.; Liu, J.; Zhang, N.C. Hydrocarbon discovery in the Ordovician dolomite reservoirs in the Maigaiti slope, Southwest Depression of the Tarim Basin, and its exploration implications. *NGIB* **2017**, *4*, 354–363. [[CrossRef](#)]
10. Chang, J.; Yang, X.; Qiu, N.S.; Min, K.; Li, C.X.; Li, H.L.; Li, D. Zircon (U-Th)/He thermochronology and thermal evolution of the Tarim Basin, Western China. *J. Asian Earth Sci.* **2022**, *230*, 105210. [[CrossRef](#)]
11. Xiao, Z.L.; Hao, Q.Q.; Shen, Z.M. Maturity Evolution of the Cambrian Source Rocks in the Tarim Basin. *Adv. Mat. Res.* **2012**, *622–623*, 1642–1645. [[CrossRef](#)]
12. Hu, G.; Meng, Q.Q.; Wang, J.; Tengger; Xie, X.M.; Lu, L.F.; Luo, H.Y.; Liu, W.H. The Original Organism Assemblages and Kerogen Carbon Isotopic Compositions of the Early Paleozoic Source Rocks in the Tarim Basin, China. *Wiley-Blackwell* **2018**, *92*, 2297–2309. [[CrossRef](#)]
13. Wu, J.Y.; He, X.Y.; Ni, X.F.; Huang, L.L. Characteristics of the Lower Cambrian Yuertus Formation source rocks in the Tarim Basin, NW China. *EES* **2019**, *360*, 12–43. [[CrossRef](#)]
14. Su, L.; Zhang, D.W.; Zheng, L.J.; Liu, X.W.; Yang, X.; Zheng, J.J.; Liu, P. Experimental study of the influences of pressure on generation and expulsion of hydrocarbons: A case study from mudstone source rocks and its geological application in the Tarim Basin. *J. Pet. Sci. Eng.* **2020**, *189*, 107021. [[CrossRef](#)]

15. Huo, Z.; Pang, X.; Ouyang, X.; Zhang, B.; Shen, W.; Guo, F.; Wang, W. Upper limit of maturity for hydrocarbon generation in carbonate source rocks in the Tarim Basin Platform, China. *Arabian J. Geosci.* **2015**, *8*, 2497–2514. [[CrossRef](#)]
16. Shen, W.B.; Pang, X.Q.; Jiang, F.J.; Zhang, B.S.; Shen, W.B.; Guo, F.T.; Wang, W.Y. Accumulation model based on factors controlling Ordovician hydrocarbons generation, migration, and enrichment in the Tazhong area, Tarim Basin, NW China. *Arabian J. Geosci.* **2016**, *9*, 347. [[CrossRef](#)]
17. Du, Z.L.; Zeng, C.M.; Qiu, H.J.; Yang, Y.X.; Zhang, L. Characteristics of two sets of Permian source rocks and oil source analysis of well Kedong 1 in Yecheng sag, southwestern Tarim Basin. *J. Jilin Univ.* **2016**, *46*, 651–660. [[CrossRef](#)]
18. Chen, J.Q.; Pang, X.Q.; Pang, H. Quantitative prediction model of present-day low-TOC carbonate source rocks: Example from the Middle-upper Ordovician in the Tarim Basin. *Energ. Explor. Exploit.* **2018**, *36*, 1335–1355. [[CrossRef](#)]
19. Anees, A.; Shi, W.Z.; Ashraf, U.; Xu, Q.H. Channel identification using 3D seismic attributes in lower Shihezi Formation of Hangjinqi area, northern Ordos Basin, China. *J. Appl. Geophys.* **2019**, *163*, 139–150. [[CrossRef](#)]
20. Ashraf, U.; Zhang, H.C.; Anees, A.; Mangi, H.N.; Tan, S.C. A core logging, machine learning and geostatistical modeling interactive approach for subsurface imaging of lenticular geobodies in a clastic depositional system, se pakistan. *Nat. Resour. Res.* **2021**, *30*, 2807–2830. [[CrossRef](#)]
21. Haitham, H.; Adam, P.; Larry, L. Prestack structurally constrained impedance inversion. *Geophysics* **2018**, *83*, 89–103. [[CrossRef](#)]
22. Ashraf, U.; Zhang, H.C.; Anees, A.; Ali, M.; Zhang, X.N.; Abbasi, S.S.; Mangi, H.N. Controls on Reservoir Heterogeneity of a Shallow-Marine Reservoir in Sawan Gas Field, SE Pakistan: Implications for Reservoir Quality Prediction Using Acoustic Impedance Inversion. *Water* **2020**, *12*, 2972. [[CrossRef](#)]
23. Anees, A.; Zhang, H.C.; Ashraf, U.; Wang, R.; Liu, K.; Mangi, H.N.; Jiang, R.; Zhang, X.N.; Liu, Q.; Tan, S.C.; et al. Identification of Favorable Zones of Gas Accumulation via Fault Distribution and Depositional facies: Insights from Hangjinqi Area, Northern Ordos Basin. *Front. Earth Sci.* **2022**, *9*, 1375. [[CrossRef](#)]
24. Anees, A.; Zhang, H.C.; Ashraf, U.; Wang, R.; Liu, K.; Abbas, A.; Ullah, Z.; Zhang, X.N.; Duan, L.Z.; Liu, F.W.; et al. Depositional facies Controls for Reservoir Quality Prediction of Lower Shihezi Member-1 of the Hangjinqi Area, Ordos Basin. *Minerals* **2022**, *12*, 126. [[CrossRef](#)]
25. Michael, P.M.; Robert, L.N.; Anne, M.T. Seismic attribute inversion for velocity and attenuation structure using data from the GLIMPCE Lake Superior experiment. *JGR* **1997**, *102*, 9949–9960. [[CrossRef](#)]
26. Thanh, H.V.; Sugai, Y.C. Integrated modelling framework for enhancement history matching in fluvial channel sandstone reservoirs. *Upstream Oil Gas Technol.* **2021**, *6*, 100027. [[CrossRef](#)]
27. Li, Y.J.; Wen, L.; Yang, H.J.; Zhang, G.Y.; Shi, J.; Peng, G.X.; Hu, J.F.; Luo, J.C.; Huang, Z.B.; Chen, Y.G. New discovery and geological significance of Late Silurian–Carboniferous extensional structures in Tarim Basin. *J. Asian Earth Sci.* **2015**, *98*, 304–319. [[CrossRef](#)]
28. Yu, J.B.; Zhang, J.; Shi, B.P. A Study on Tectono-Thermal Evolution History of Bachu Uplift in the Tarim Basin. *Chin. J. Geophys.* **2010**, *53*, 805–814. [[CrossRef](#)]
29. Zhou, X.B.; Li, J.H.; Li, W.S.; Cheng, Y.L.; Wang, H.H. Tectonic Units Division of Crystalline Basement in the Tarim Basin, NW China. *Acta Geol. Sin.* **2015**, *89*, 127. [[CrossRef](#)]
30. Neng, Y.; Wu, G.H.; Huang, S.Y.; Zhang, X.; Cao, S.J. Formation stage and controlling factors of the paleo-uplifts in the Tarim Basin: A further discussion. *NGIB* **2016**, *3*, 209–215. [[CrossRef](#)]
31. Wang, Z.Y.; Gao, Z.Q.; Fan, T.L.; Zhang, H.H.; Yuan, Y.X.; Wei, D.; Qi, L.X.; Yun, L.; Karubandika, G.M. Architecture of strike-slip fault zones in the central Tarim Basin and implications for their control on petroleum systems. *J. Pet. Sci. Eng.* **2022**, *213*, 110432–114032. [[CrossRef](#)]
32. Zhang, J.L.; Zhang, Z.J. Depositional facies of the Silurian tide-dominated paleo-estuary of the Tazhong area in the Tarim Basin. *Pet. Sci.* **2008**, *5*, 95–104. [[CrossRef](#)]
33. Lin, C.S.; Yang, H.J.; Liu, J.Y.; Peng, L.; Cai, Z.Z.; Yang, X.F.; Yang, Y.H. Paleogeomorphology of the Paleozoic central uplift belt and its constraint on the development of depositional facies in the Tarim Basin. *Sci. China Earth Sci.* **2009**, *52*, 823–834. [[CrossRef](#)]
34. Liu, K.N.; Jiang, Z.X.; Zhong, D.K.; Kang, R.; Cao, Y. Study on Depositional facies of Carboniferous Kalashayi Formation in the South of Tahe Oilfield. *Adv. Mat. Res.* **2012**, *433*, 1745–1750. [[CrossRef](#)]
35. Ma, B.B.; Lu, Y.C.; Eriksson, K.A.; Peng, L.; Xing, F.C.; Li, X.Q. Multiple organic–inorganic interactions and influences on heterogeneous carbonate-cementation patterns: Example from Silurian deeply buried sandstones, central Tarim Basin, north-western China. *Sedimentology* **2020**, *68*, 670–696. [[CrossRef](#)]
36. Kassem, A.A.; Hussein, W.S.; Radwan, A.E.; Anani, N.; Abioui, M.; Jain, S.; Shehata, A.A. Petrographic and diagenetic study of siliciclastic Jurassic sediments from the northeastern margin of Africa: Implication for reservoir quality. *J. Petrol. Sci. Eng.* **2021**, *200*, 108340. [[CrossRef](#)]
37. Kassem, A.A.; Osman, O.; Nabawy, B.; Baghdady, A.R.; Shehata, A.A. Microfacies Analysis and Reservoir Discrimination of Channelized Carbonate Platform Systems: An Example from the Turonian Wata Formation, Gulf of Suez, Egypt. *J. Petrol. Sci. Eng.* **2022**, *212*, 110272. [[CrossRef](#)]
38. Liu, L.F.; Qiao, J.Q.; Shen, B.J.; Lu, X.Y.; Yang, Y.S. Geological characteristics and shale gas distribution of carboniferous mudstones in the Tarim Basin, China. *Acta Geochim.* **2017**, *36*, 260–275. [[CrossRef](#)]

39. Cheng, B.; Chen, Z.H.; Chang, X.C.; Chang, X.C.; Yang, F.L. Biodegradation and possible source of Silurian and Carboniferous reservoir bitumens from the Halahatang sub-depression, Tarim Basin, NW China. *Mar. Pet. Geol.* **2016**, *78*, 236–246. [[CrossRef](#)]
40. Meng, M.M.; Fan, T.L. Sedimentary characteristics and formation mechanisms of the Ordovician carbonate shoals in the Tarim Basin, NW China. *Carbonates Evaporites* **2020**, *35*, 47–77. [[CrossRef](#)]
41. Jiang, D.H.; Yan, S.J.; Pu, R.H.; Su, S.Y.; Zhou, F.; Chen, Q.L. Coal and shale distributions on half-graben slopes: A case study of the Eocene Pinghu Formation in Xihu Sag, East China Sea. *Interpretation* **2022**, *10*, 1–11. [[CrossRef](#)]
42. Ashraf, U.; Zhu, P.M.; Yasin, Q.; Anees, A.; Imraz, M.; Mangi, H.N.; Shakeel, S. Classification of reservoir facies using well log and 3D seismic attributes for prospect evaluation and field development: A case study of Sawan gas field, Pakistan. *J. Petro. Sci. Eng.* **2019**, *175*, 338–351. [[CrossRef](#)]
43. Mukhopadhyay, P.K.; Wade, J.A.; Kruger, M.A. Organic facies and maturation of Jurassic/Cretaceous rocks, and possible oil-source rock correlation based on pyrolysis of asphaltene, Scotian Basin, Canada. *Org. Geochem.* **1995**, *22*, 85–104. [[CrossRef](#)]
44. Pu, R.H. Geological interpretation of progradational reflection. *Oil Geophys. Prospect.* **1994**, *29*, 490–497.
45. Gu, J.Y. A Study of Sedimentary Environment and Reservoir Quality of the Carboniferous Donghe Sandstone in the Tarim Basin. *Acta Geo. Sin-Engl.* **2009**, *9*, 395–406. [[CrossRef](#)]
46. Lüthje, C.J.; Nichols, G.; Jerrett, R. Depositional facies and reconstruction of a transgressive coastal plain with coal formation, Paleocene, Spitsbergen, Arctic Norway. *NJG* **2020**, *100*, 1–49. [[CrossRef](#)]
47. Laurent, G.C.; Edoardo, P.; Ian, S.R.; Peacock, D.C.P.; Roger, S.; Ragnar, P.; Hercinda, F.; Vladimir, M. Origin and diagenetic evolution of gypsum and microbialitic carbonates in the Late Sag of the Namibe Basin (SW Angola). *Sediment. Geol.* **2016**, *342*, 13–115. [[CrossRef](#)]